1

General Background of Carbon Materials

1.1 Carbon Allotrope

Carbon (atomic number 6) is one of the most abundant elements on Earth, with a Clarke number of 14. As a fundamental component of all living organisms, carbon plays a crucial role in both natural and synthetic materials. Unlike most elements, carbon exhibits an extraordinary diversity of allotropes, each with distinct structural and physical properties. A comprehensive database of carbon allotropes is available, cataloging their crystallographic structures and properties [1]. These allotropes can be classified based on the hybridization state of their carbon atoms, as outlined in the following text, providing a framework for understanding their structural variations and potential applications.

1.1.1 sp^3-Carbon Allotropes

Among the carbon allotropes composed of sp^3-hybridized carbon atoms, cubic diamond (Figure 1.1a) is the most well known. Diamond is one of the hardest naturally occurring materials on Earth. It exhibits exceptional properties, including transparency, electrical insulation, high thermal conductivity, and chemical stability. Due to these characteristics, diamond is highly valued not only as a gemstone, but also as industrial material for applications, such as abrasives and heat dissipation components. Additionally, boron- or phosphorus-doped diamond has been widely used in semiconductor devices and corrosion-resistant electrodes.

Furthermore, under extreme conditions, such as meteorite impacts or ultrahigh-pressure environments, the formation of hexagonal diamond (lonsdaleite) has been reported (Figure 1.1b) [2, 3]. However, only minute quantities have been obtained, and its physical properties remain largely unexplored experimentally. In addition to these known structures, several other sp^3-carbon allotropes, such as T-carbon [4], have also been theoretically predicted.

1.1.2 sp^2-Carbon Allotropes

Each sp^2-hybridized carbon atom can form bonds with three adjacent atoms. Among the possible structures based on the sp^2-hybridized carbon configuration, the most

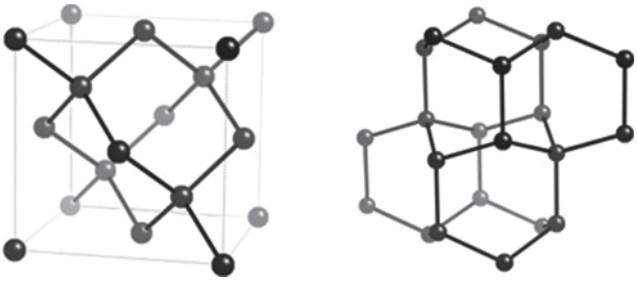

Figure 1.1 Structures of (a) cubic diamond (https://next-gen.materialsproject.org/materials/mp-66) and (b) hexagonal diamond (https://legacy.materialsproject.org/materials/mp-47/).

symmetric and fundamental geometric unit is the hexagon. As a result, graphene represents the thermodynamically most stable sp^2-carbon allotrope, consisting of two-dimensional (2D) networks of hexagonally arranged carbon atoms. Throughout this book, we will refer to a single graphene sheet simply as graphene, whereas stacked sheets are treated separately, as described in Chapter 2. However, carbon networks in which each carbon atom is bonded to three neighboring carbon atoms are not limited to hexagonal arrangements; they can also incorporate pentagons, heptagons, and octagons. As shown in Figure 1.2, different combinations of these polygonal units form a variety of fundamental building blocks for complex carbon structures.

When 20 hexagons and 12 pentagons assemble in an alternating fashion, they form a spherical carbon molecule known as fullerene, exemplified by C_{60} (Figure 1.2a) [7]. When additional hexagons are introduced while maintaining the number of pentagons, higher fullerenes such as C_{70}, C_{76}, C_{78}, and C_{84} can be obtained [8]. Fullerenes are capable of forming multilayered structures [9], and when multiple layers are stacked concentrically, they are referred to as onion-like carbons or carbon nano-onions (Figure 1.2a) [5, 10].

As shown in Figure 1.2b, a material obtained by formally rolling a graphene sheet into a cylindrical form is known as carbon nanotubes (CNTs) [11, 12]. CNTs exhibit numerous isomeric forms depending on their diameter and chirality, which is defined by chiral vector and includes armchair and zigzag. These structural parameters determine whether they exhibit metallic or semiconducting properties [13]. CNTs can also form multiwalled structures, known as multiwalled carbon nanotubes (MWCNTs) [12, 14]. When the stacking number is further increased and diameter increases beyond several hundred nanometers, these structures are referred to as carbon nanofibers (CNFs) [6], and when the diameter exceeds several micrometers, they are classified as carbon fibers. In this book, CNT-related materials are introduced in the order of single-walled carbon nanotubes (SWCNTs), MWCNTs, and CNFs to facilitate the reader's understanding. However, historically, carbon fibers were the first to be developed, followed by the emergence of CNFs [15] (also referred to as carbon filaments [16]), MWCNTs [12], and finally, SWCNTs [11].

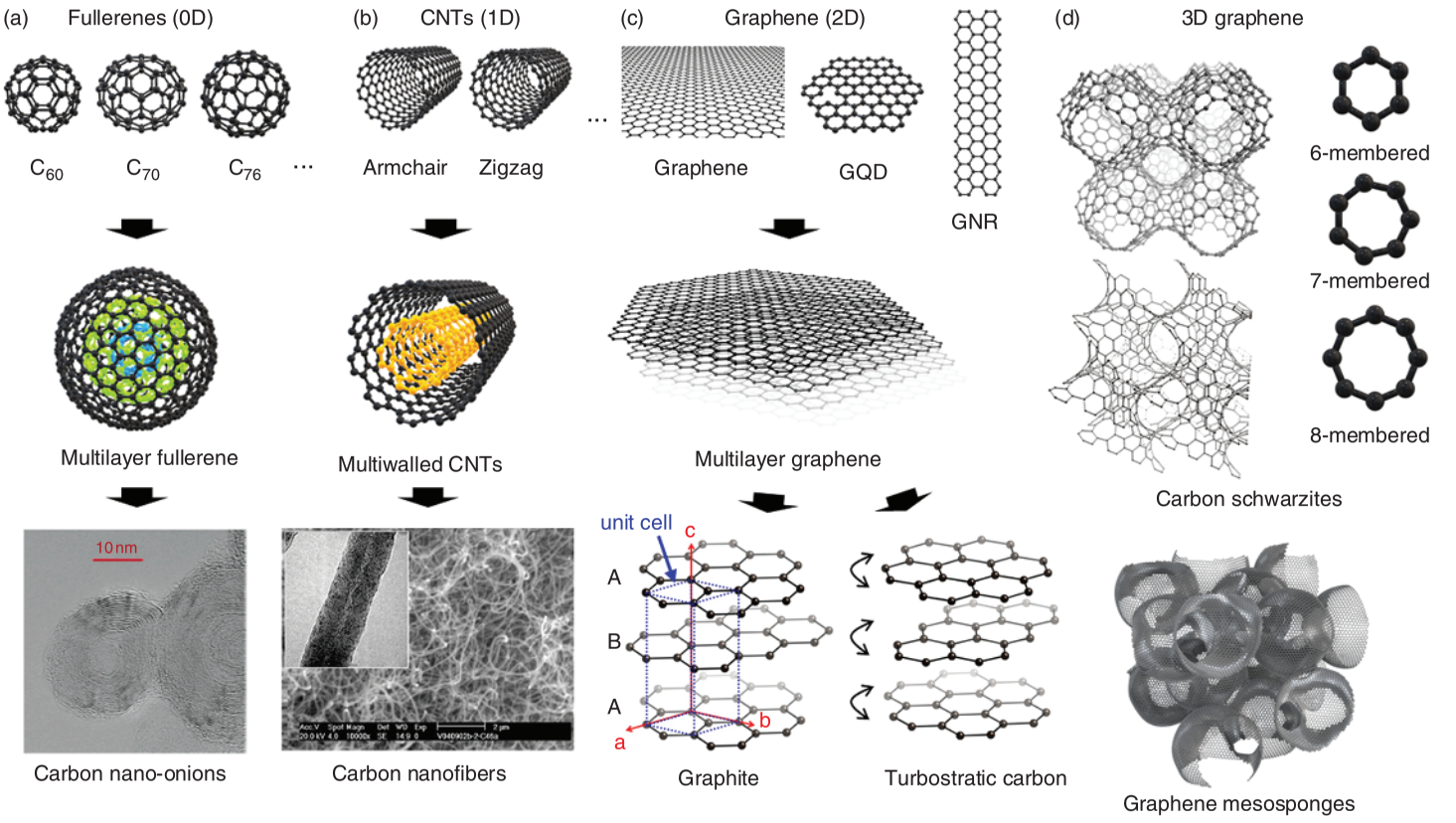

Figure 1.2 (a–c) Major building blocks of sp^2-carbon allotropes: (a) fullerenes (0D), (b) CNTs (1D), and (c) graphene (2D), each shown with their respective multilayered forms. The bottom panels of (a) and (b) are from Ref. [5] / with permission of the American Chemical Society) and Ref. [6] / with permission of Elsevier. The bottom panel of (c) illustrates two types of stacking configurations in multilayer graphene: ABA stacking (left) typical of graphite and turbostratic stacking (right) with rotated basal planes. (d) 3D graphene frameworks: carbon schwarzites (top) featuring characteristic 6-, 7-, and 8-membered carbon rings, and graphene mesosponge (bottom). All materials except carbon schwarzites were experimentally synthesized.

The presence of 1D periodicity in carbon materials led to the emergence of outstanding physicochemical, thermomechanical, and electrochemical properties of covalently functionalized SWCNTs in a variety of energy-related applications. These include photocatalysis [17, 18], solar cell [19–21], field-effect transistor [22, 23], gas and biosensors [24, 25], and nanomechanical oscillators [26, 27], in addition to various electrochemical applications [28, 29].

Graphene is a 2D material consisting of a single atomic layer of carbon hexagonal networks (Figure 1.2c) [30]. While graphene has long been recognized as the fundamental building unit of graphite, isolating an individual graphene sheet remained challenging due to the strong interlayer van der Waals interactions arising from π–π stacking. It was only relatively recently that single-layer graphene was successfully exfoliated [31]. Graphene exhibits extraordinary physical and chemical properties, making it one of the most remarkable materials in modern science. It has an intrinsic tensile strength of approximately $42\,N\,m^{-1}$, surpassing that of steel with the corresponding thickness (approximately $0.13 - 0.18\,N\,m^{-1}$) by more than an order of magnitude, and an elastic modulus of around 1 TPa, demonstrating exceptional mechanical robustness [32]. In terms of electrical properties, graphene possesses an electron mobility exceeding $200{,}000\,cm^2\,V^{-1}\,s^{-1}$ at room temperature [33], significantly higher than that of silicon (approximately $1{,}400–1{,}500\,cm^2\,V^{-1}\,s^{-1}$), enabling its potential for high-speed electronic applications. Additionally, graphene displays exceptional thermal conductivity, reaching values above $5{,}000\,W\,m^{-1}\,K^{-1}$ [34], making it one of the best known thermal conductors. Its optical transparency is also remarkable, as a monolayer graphene sheet absorbs only 2.3% of visible light [35]. These unique characteristics position graphene as a highly promising material for applications in nanoelectronics, energy storage, sensors, and flexible devices. Moreover, graphene has various derivatives depending on its size and shape. Narrow ribbon-like structures are known as graphene nanoribbons (GNRs) [36, 37], while small fragments with dimensions below a few nanometers are referred to as graphene nanodots or graphene quantum dots (GQDs) [38, 39] (Figure 1.2c). These nanostructures introduce a bandgap into graphene, which is originally a Dirac semimetal with zero bandgap, due to quantum confinement effects [40].

When two graphene layers are stacked, the resulting structure is referred to as bilayer graphene [41]. It is well established that the physical properties of bilayer graphene vary significantly depending on the stacking angle between the layers [42]. When multiple layers of graphene are stacked, the material is termed multilayer graphene. As the number of layers increases, the characteristics of multilayer graphene gradually converge toward those of graphite. Graphite is the most well-known, naturally occurring allotrope composed of sp^2-hybridized carbon. As illustrated in Figure 1.2c, the crystalline structure of graphite consists of periodically stacked graphene layers. A detailed examination of this stacking arrangement reveals that if one graphene layer is designated as the A layer, the adjacent B layer exhibits a slight in-plane displacement of its carbon atoms. Furthermore, the subsequent A' layer aligns with the initial A layer when viewed along the direction perpendicular to the hexagonal plane. This repeating $A \rightarrow B \rightarrow A \rightarrow B$ stacking sequence forms the structure known as the ABA configuration, or hexagonal

graphite structure. While graphite is classified as a crystal, as it possesses a well-defined unit cell (Figure 1.2c), not all carbon materials exhibit such regular stacking. When graphene sheets do not follow the ABA stacking order and instead adopt a random rotational misalignment between layers (Figure 1.2c), the resulting carbon material is referred to as turbostratic carbon [43]. This type of carbon serves as a primary structural component in various carbon materials, including activated carbons, carbon blacks, glassy carbons, and carbon fibers.

It is important to recognize that the terms fullerenes, CNTs, and graphenes do not refer to single, well-defined materials but rather encompass a broader class of structures based on graphene sheets arranged in different dimensional forms: zero-dimensional (0D) spheres, 1-dimensional (1D) tubes, and 2-dimensional (2D) sheets (Figure 1.2). These fundamental sp^2-bonded carbon structures serve as the primary building blocks for a diverse range of carbon nanomaterials and constitute the family of sp^2-carbon allotropes. Their structural variations enable tunable electronic, mechanical, and chemical properties, making them highly versatile for applications in electronics, energy storage, catalysis, and advanced composites. It should be noted, from a macroscopic perspective, that discrete π-conjugated molecules can be considered as 0D materials. Accordingly, in this book, large sp^2-conjugated molecules such as cycloparaphenylenes (CPPs) [44, 45] and warped nanographene [46] are also regarded as 0D carbons.

For a long time, graphite, which comprises stacked layers of 2D graphene, was the only known allotrope of sp^2-hybridized carbon except amorphous carbons. However, the discovery of 0D fullerenes in 1985 [7] and 1D CNTs in 1991 [12] broadened the understanding that sp^2-carbon networks could exist across multiple dimensions. Naturally, this recognition led researchers to explore the possibility of three-dimensional (3D) sp^2-carbon architectures. While CNTs and graphene can be constructed solely from hexagonal carbon networks, the incorporation of pentagons induces positive Gaussian curvature, enabling the formation of closed, curved structures. According to Euler's theorem, 12 pentagons are required to fully enclose a carbon framework, as seen in fullerenes. Conversely, the introduction of heptagons or octagons imparts negative Gaussian curvature, yielding saddle-shaped surfaces. These geometric considerations suggest the feasibility of constructing continuous 3D carbon frameworks composed entirely of sp^2-carbon atoms [47]. Among these structures, particular interest has been directed toward Schwarz minimal surfaces, a class of mathematically defined surfaces characterized by their triply periodic minimal geometry (Figure 1.2d, top). Researchers have explored the possibility of realizing such structures by envisioning novel 3D sp^2-carbon networks with unique electronic and mechanical properties, called carbon schwarzites [48]. Efforts to synthesize carbon schwarzites have persisted for over three decades, with numerous studies reported in the literature. However, a perfect synthesis achieving an ideal crystalline structure has yet to be accomplished. Nevertheless, even if a fully ordered crystalline form remains elusive, a material composed of curved monolayer graphene, forming a continuous structure without exposed graphene edges (edge sites), could still exhibit many of the highly desirable properties anticipated for 3D graphene. This concept has

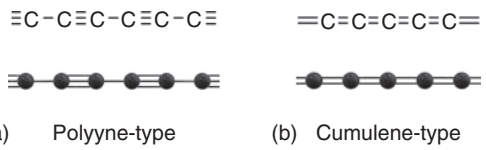

Figure 1.3 Structures of carbynes. (a) polyyne-type and (b) cumulene-type. The number of carbon atoms shown is illustrative and intended to represent extended one-dimensional chains rather than specific molecular sizes.

guided the development of novel materials, including the graphene mesosponge (GMS; Figure 1.2d, bottom) [49], which will be discussed in detail in Chapter 5 of this book.

1.1.3 *sp*-Carbon Allotropes

Carbyne is a unique 1D carbon allotrope composed entirely of *sp*-hybridized carbon atoms, forming a linear chain structure [50]. It can exist in two distinct bonding configurations: the polyyne-type (Figure 1.3a), characterized by alternating single and triple bonds (—C≡C—C≡), and the cumulene-type (Figure 1.3b), consisting of consecutive double bonds (=C=C=C=). Carbyne is predicted to exhibit unique mechanical, electronic, and optical properties, which are different from diamond and graphite. However, its extreme instability under ambient conditions has significantly hindered experimental studies, as it readily crosslinks into more stable carbon phases such as graphite. Despite these challenges, recent advances in chemical synthesis, encapsulation within CNTs [51], and high-pressure techniques have enabled the fabrication of carbyne chains in controlled environments. While its large-scale synthesis and stabilization remain unsolved challenges, carbyne's remarkable theoretical properties continue to drive research interest.

1.1.4 Carbon Allotropes Consisting of Multiple Carbon Hybridization States

In addition to the carbon allotropes composed solely of sp^3-, sp^2-, or *sp*-hybridized carbon atoms, allotropes exist that are formed by the combination of carbon atoms with different hybridization states. Material composed of a mixture of sp^3- and sp^2-hybridized carbon atoms is known as diamond-like carbons (DLCs), exhibiting a unique combination of diamond-like hardness and graphite-like electrical conductivity [52]. The proportion of sp^3 content determines its mechanical and electronic properties, with higher sp^3 fractions leading to greater hardness and wear resistance. DLC films are widely used as protective coatings in various industries, including automotive, biomedical, and electronics, due to their exceptional properties such as high hardness, low friction, chemical inertness, and biocompatibility. Advanced deposition techniques, such as plasma-enhanced chemical vapor deposition [53] and sputtering [54], enable precise control over the structural and functional characteristics of DLC, expanding its applications in emerging fields such as wear-resistant coatings for medical implants and high-performance electronic devices.

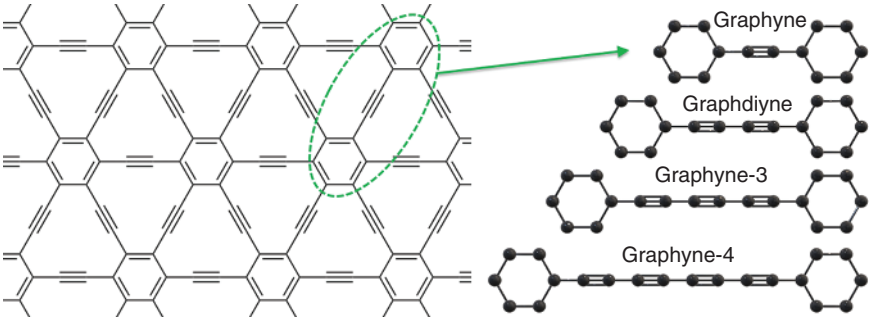

Figure 1.4 Representative examples for graphyne and related materials.

Graphyne and graphdiyne are emerging carbon allotropes that extend the structural diversity of sp^2-carbon networks by incorporating *sp*-hybridized carbon atoms (Figure 1.4) [55]. Unlike graphene, which consists solely of sp^2-hybridized carbon in a hexagonal lattice, these materials feature alternating *sp*- and sp^2-hybridized bonds, introducing acetylenic (—C≡C—) linkages between hexagonal carbon units. Graphyne consists of single acetylenic linkages, whereas graphdiyne contains diacetylenic (—C≡C—C≡C—) connections. Furthermore, the acetylene linkage can be extended even further (Figure 1.4), leading to increased porosity and tunable electronic properties. These unique characteristics provide graphyne and the related materials with potential advantages over conventional graphene-based materials, particularly in applications requiring adjustable band gaps, high carrier mobility, and porous structures for molecular sieving, energy storage, and catalysis. Despite significant theoretical predictions of their superior properties [56], experimental synthesis remains a challenge, with current methods producing limited quantities of these materials. Nevertheless, continued advancements in synthetic strategies are expected to unlock their full potential in next-generation electronic and energy devices.

1.2 Synthesis of sp^2-Based Carbon Allotropes

As previously discussed in the given chapter, carbon exhibits a wide variety of allotropes, each of which has been the subject of extensive and intriguing research due to their diverse structures and properties. In this book, we focus specifically on 3D structures composed of sp^2 carbon, particularly 3D graphene (Figure 1.2d). To gain a deeper understanding of the synthesis strategies, anticipated properties, and potential functionalities of 3D graphene, this section provides an overview of the fundamental synthesis methods of sp^2-carbon materials.

When organic compounds are heated under an inert atmosphere at ambient or lower pressures, noncarbon elements such as hydrogen and oxygen are volatilized, leading to the concentration of carbon and the formation of sp^2-carbon materials. This transformation process is well illustrated by "Iceberg Model" (Figure 1.5) proposed by Ohtani [57], which effectively depicts how various organic precursors can be converted into carbon materials as their carbon concentration increases.

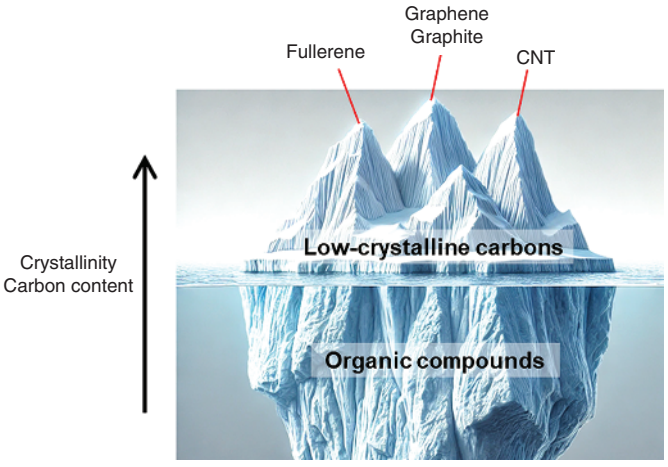

Figure 1.5 The "Iceberg Model" for carbon materials. The original illustration [57] has been adapted and stylized to fit the context of this book.

Despite the vast diversity of organic compounds, any precursor can ultimately yield carbon materials once the carbon content is sufficiently enriched. When the carbon concentration exceeds approximately 90%, the material is generally considered a carbon material (corresponding to the region above the water surface in the Iceberg Model). However, these materials exhibit a wide range of crystallinity, from low-crystalline to highly crystalline structures. Low-crystallinity carbon materials include charcoal, activated carbon, carbon fibers, carbon black, and glassy carbon. By increasing crystallinity through high-temperature treatment or catalytic processes, these materials can be further refined, eventually forming highly ordered structures such as fullerenes, CNTs, graphene, and graphite.

As illustrated by the 'Iceberg Model', there are countless pathways for synthesizing sp^2-carbon materials from organic compounds, reflecting the enormous diversity of organic precursors, and numerous methods have been proposed over the years. These synthesis routes can be broadly classified into solid-phase carbonization, liquid-phase carbonization, and gas-phase carbonization, depending on the physical state of the precursor during the transformation process. Thus, understanding the fundamental principles behind these carbonization mechanisms is crucial for developing effective sp^2-carbon synthesis strategies as it allows for precise control over the structures, crystallinity, and functional properties of the resulting materials.

1.2.1 Solid-Phase Carbonization

When pieces of wood or plants are pyrolyzed under oxygen-deficient conditions at high temperatures, they transform into charcoal, one of the earliest carbon materials used by humankind. Charcoal retains the original morphology of the wood precursor due to the 3D cross-linked structure of lignin, which, upon carbonization, forms an intricate network of interconnected graphene sheets. This process, where

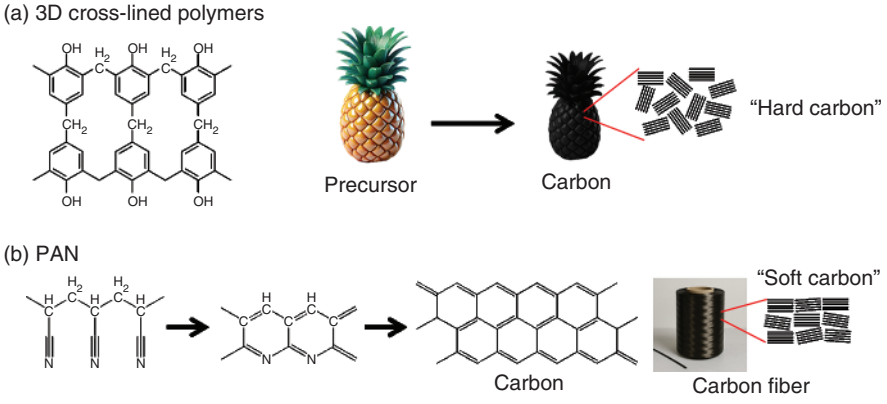

Figure 1.6 Schematic illustrations of solid-phase carbonization processes for (a) 3D cross-linked polymers and (b) polyacrylonitrile (PAN).

a solid precursor is converted into carbon while maintaining its shape, is known as solid-phase carbonization (Figure 1.6a). While the overall morphology is preserved, a slight volume shrinkage typically occurs. Similarly, thermosetting polymers, such as phenolic resins and furan resins, which possess 3D cross-linked networks, are widely used as precursors for carbon materials that retain their original shape *via* solid-phase carbonization. Carbon derived from these polymers consists of graphene sheets randomly arranged and often interlinked, making it difficult to convert into graphite even at temperatures exceeding 2,000 °C. This type of carbon is referred to as *hard carbon*, characterized by its high structural disorder and resistance to graphitization. Hard carbon is of significant importance as an anode material in lithium-ion and sodium-ion batteries, offering high capacity and structural stability [58].

In addition to resins with 3D cross-linking, polyacrylonitrile (PAN) is another widely used precursor for solid-phase carbonization, particularly in the production of carbon fibers (Figure 1.6b) and graphite sheets. Unlike lignin-based materials, PAN does not initially possess a 3D cross-linked structure, but during thermal decomposition, it undergoes structural transformation into graphene-like layers, making it a graphitizable carbon, commonly referred to as *soft carbon*. When PAN fibers are heat treated at high temperatures, they yield highly crystalline, high-strength carbon fibers, which are extensively used in aerospace, automotive, and high-performance composite applications.

1.2.2 Liquid-Phase Carbonization

When thermoplastic polymers, such as polyvinyl chloride or polyvinyl alcohol, are heated, they undergo thermal decomposition above 200 °C, transitioning into pitch, a complex mixture of polycyclic aromatic hydrocarbons (Figure 1.7). At around 300 °C, pitch remains in a liquid state, but as the temperature increases further, it solidifies, ultimately transforming into a sp^2-carbon material. This process, in which the precursor material passes through a liquid phase before carbonization, is

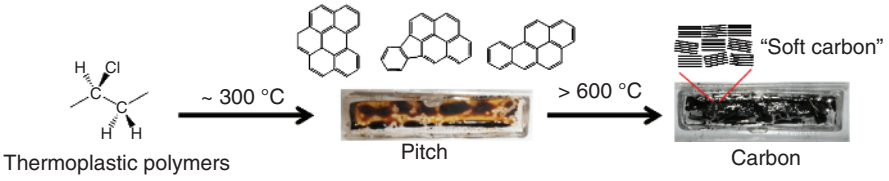

Figure 1.7 Schematic illustration of liquid-phase carbonization.

referred to as liquid-phase carbonization. The structural characteristics of the liquid precursor are largely retained in the final carbon material. Instead of synthesizing pitch *in situ*, coal tar pitch and similar materials can also be directly used as precursors. Because liquid carbon precursors can easily infiltrate the nanopores of template materials, such as oxide ceramics [59], templating techniques are commonly used to achieve precise control over the nanostructure of the resulting carbon materials. Specifically, mesoporous oxide ceramics and oxide ceramic nanoparticles are frequently used as templates to guide the formation of well-defined carbon nanostructures. Additionally, since polycyclic aromatic hydrocarbons in pitch exhibit a high degree of parallel alignment, the resulting carbon material tends to be soft carbon, which can be further processed to enhance its graphitic structure.

1.2.3 Gas-Phase Carbonization

Gas-phase carbonization refers to the thermal decomposition of gaseous carbon precursors, such as hydrocarbon gases and alcohols, at high temperatures, leading to the formation of carbon materials. This method is widely used in industrial production, particularly for carbon black. In the flame method (Figure 1.8a), hydrocarbon gases such as acetylene and vaporized liquid fuels are fed into a burner, where combustion generates soot, which consists of interconnected spherical carbon black nanoparticles. In the absence of catalysts, hydrocarbons decompose thermally, resulting in the formation of these nanocarbon aggregates. Fullerenes can also be synthesized using a similar flame-based approach.

In contrast, when carbon precursor gases are thermally decomposed without direct combustion, the process is referred to as chemical vapor deposition (CVD) (Figure 1.8b). Catalyst-free CVD, where a hydrocarbon source undergoes pyrolysis and deposits carbon onto a substrate, is used in the synthesis of highly oriented pyrolytic graphite (HOPG) and molecular sieving carbons. Meanwhile, catalyst-assisted CVD, using transition metals or oxide ceramics, enables the controlled synthesis of nanostructured carbon materials, such as CNTs and graphene. In particular, catalytic CVD with nanoporous oxide ceramic templates has emerged as a promising strategy for fabricating 3D graphene architectures with highly controlled nanostructures [60]. One of the close-to-genuine 3D graphene materials introduced in this book, graphene mesosponge [49], is synthesized using an oxide ceramic-catalyzed CVD process, enabling precise structural control and enhanced material properties.

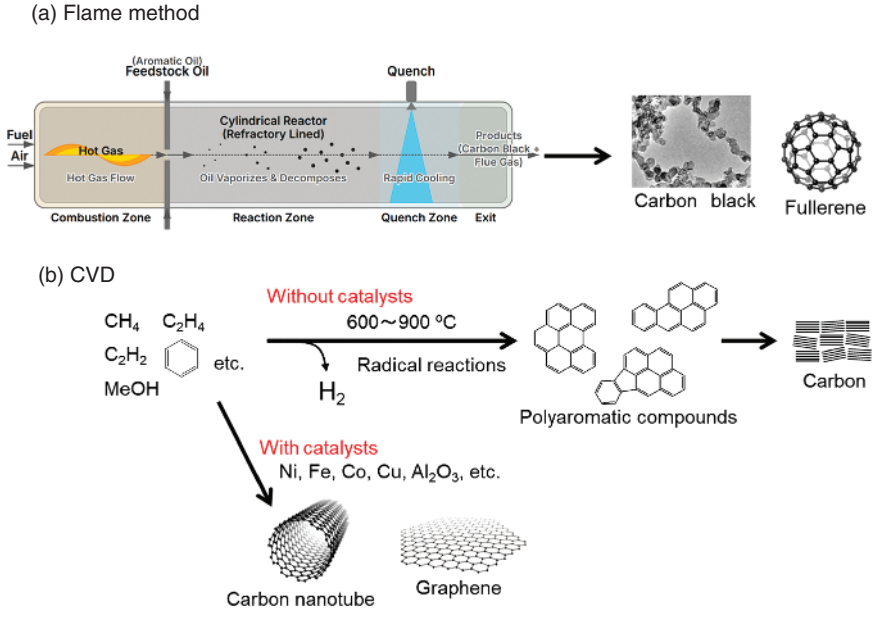

Figure 1.8 Schematic illustration of gas-phase carbonization. (a) Flame method. (b) Chemical vapor deposition (CVD).

References

1 Samara Carbon Allotrope Database (SACADA). https://www.sacada.info/ (accessed 12 January 2026).

2 Frondel, C. and Marvin, U.B. (1967). Lonsdaleite, a hexagonal polymorph of diamond. *Nature* 214: 587–589.

3 Bundy, F.P. and Kasper, J.S. (1967). Hexagonal diamond – a new form of carbon. *J. Chem. Phys.* 46: 3437–3446.

4 Sheng, X.-L., Yan, Q.-B., Ye, F. et al. (2011). T-carbon: a novel carbon allotrope. *Phys. Rev. Lett.* 106: 155703.

5 Ding, L., Stilwell, J., Zhang, T. et al. (2005). Molecular characterization of the cytotoxic mechanism of multiwall carbon nanotubes and nano-onions on human skin fibroblast. *Nano Lett.* 5: 2448–2464.

6 Hammel, E., Tang, X., Trampert, M. et al. (2004). Carbon nanofibers for composite applications. *Carbon* 42: 1153–1158.

7 Kroto, H.W., Heath, J.R., Obrien, S.C. et al. (1985). C_{60}: buckminsterfullerene. *Nature* 318: 162–163.

8 Ajie, H., Alvarez, M.M., Anz, S.J. et al. (1990). Characterization of the soluble all-carbon molecules C_{60} and C_{70}. *J. Phys. Chem.* 94: 8630–8633.

9 Maiti, A., Brabec, C.J., and Bernholc, J. (1993). Structure and energetics of single and multilayer fullerene cages. *Phys. Rev. Lett.* 70: 3023–3026.

10 Pech, D., Brunet, M., Durou, H. et al. (2010). Ultrahigh-power micrometre-sized supercapacitors based on onion-like carbon. *Nat. Nanotechnol.* 5: 651–654.

11 Iijima, S. and Ichihashi, T. (1993). Single-Shell carbon nanotubes of 1-nm diameter. *Nature* 363: 603–605.

12 Iijima, S. (1991). Helical microtubules of graphitic carbon. *Nature* 354: 56–58.

13 Saito, R., Dresselhaus, G., and Dresselhaus, M.S. (1996). Tunneling conductance of connected carbon nanotubes. *Phys. Rev. B* 53: 2044–2050.

14 Iijima, S., Brabec, C., Maiti, A., and Bernholc, J. (1996). Structural flexibility of carbon nanotubes. *J. Chem. Phys.* 104: 2089–2092.

15 Endo, M. and Kroto, H.W. (1992). Formation of carbon nanofibers. *J. Phys. Chem.* 96: 6941–6944.

16 Baker, R.T.K. (1989). Catalytic growth of carbon filaments. *Carbon* 27: 315–323.

17 González-Muñoz, D., Martín-Somer, A., Strobl, K. et al. (2021). Enhancing visible-light photocatalysis via endohedral functionalization of single-walled carbon nanotubes with organic dyes. *ACS Appl. Mater. Interfaces* 13: 24877–24886.

18 Nova-Fernández, J.L., González-Muñoz, D., Pascual-Coca, G. et al. (2024). Enhancing the photocatalytic activity via direct covalent functionalization in single-walled carbon nanotubes. *Adv. Funct. Mater.* 34: 13.

19 I. Jeon, Matsuo, Y., and Maruyama, S. (2018). Single-walled carbon nanotubes in solar cells. *Top. Curr. Chem.* 376: 28.

20 Muchuweni, E., Mombeshora, E.T., Martincigh, B.S., and Nyamori, V.O. (2022). Recent applications of carbon nanotubes in organic solar cells. *Front. Chem.* 9: 16.

21 Patel, K., Prochowicz, D., Akin, S. et al. (2023). Applications of carbon-based materials for improving the performance and stability of perovskite solar cells. *Energ. Technol.* 11: 28.

22 Islam, A.E. (2013). Variability and reliability of single-walled carbon nanotube field effect transistors. *Electronics* 2: 332–367.

23 Bishop, M.D., Hills, G., Srimani, T. et al. (2020). Fabrication of carbon nanotube field-effect transistors in commercial silicon manufacturing facilities. *Nat. Electron.* 3: 492–501.

24 Dewey, H.M., Lamb, A., and Budhathoki-Uprety, J. (2024). Recent advances on applications of single-walled carbon nanotubes as cutting-edge optical nanosensors for biosensing technologies. *Nanoscale* 16: 16344–16375.

25 Guo, S.Y., Hou, P.X., Zhang, F. et al. (2022). Gas sensors based on single-wall carbon nanotubes. *Molecules* 27: 22.

26 Shi, J.X., Lei, X.W., and Natsuki, T. (2021). Review on carbon nanomaterials-based nano-mass and nano-force sensors by theoretical analysis of vibration behavior. *Sensors* 21: 20.

27 Li, C.Y. and Chou, T.W. (2003). Single-walled carbon nanotubes as ultrahigh frequency nanomechanical resonators – art. no. 073405. *Phys. Rev. B* 68: 3.

28 Sirisinudomkit, P., Senokos, E., Rubio, N., and Shaffer, M.S.P. (2021). Reductive processing of single walled carbon nanotubes for high volumetric performance supercapacitors. *Mater. Adv.* 2: 1981–1992.

29 Zheng, Y.J., Dai, W.Y., Zhang, X.Q. et al. (2022). Nanotube-based heterostructures for electrochemistry: a mini-review on lithium storage, hydrogen evolution and beyond. *J. Energy Chem.* 70: 630–642.

30 Geim, A.K. and Novoselov, K.S. (2007). The rise of graphene. *Nat. Mater.* 6: 183–191.

31 Novoselov, K.S., Geim, A.K., Morozov, S.V. et al. (2004). Electric field effect in atomically thin carbon films. *Science* 306: 666–669.

32 Lee, C., Wei, X., Kysar, J.W., and Hone, J. (2008). Measurement of the elastic properties and intrinsic strength of monolayer graphene. *Science* 321: 385–388.

33 Bolotin, K.I., Sikes, K.J., Jiang, Z. et al. (2008). Ultrahigh electron mobility in suspended graphene. *Solid State Commun.* 146: 351–355.

34 Balandin, A.A., Ghosh, S., Bao, W. et al. (2008). Superior thermal conductivity of single-layer graphene. *Nano Lett.* 8: 902–907.

35 Nair, R.R., Blake, P., Grigorenko, A.N. et al. (2008). Fine structure constant defines visual transparency of graphene. *Science* 320: 1308–1308.

36 Nakada, K., Fujita, M., Dresselhaus, G., and Dresselhaus, M.S. (1996). Edge state in graphene ribbons: nanometer size effect and edge shape dependence. *Phys. Rev. B* 54: 17954–17961.

37 Son, Y.-W., Cohen, M.L., and Louie, S.G. (2006). Energy gaps in graphene nanoribbons. *Phys. Rev. Lett.* 97: 216803.

38 Trauzettel, B., Bulaev, D.V., Loss, D., and Burkard, G. (2007). Spin qubits in graphene quantum dots. *Nat. Phys.* 3: 192–196.

39 Ponomarenko, L.A., Schedin, F., Katsnelson, M.I. et al. (2008). Chaotic Dirac billiard in graphene quantum dots. *Science* 320: 356–358.

40 Berger, C., Song, Z., Li, X. et al. (2006). Electronic confinement and coherence in patterned epitaxial graphene. *Science* 312: 1191–1196.

41 Novoselov, K.S., McCann, E., Morozov, S.V. et al. (2006). Unconventional quantum Hall effect and Berry's phase of 2π in bilayer graphene. *Nat. Phys.* 2: 177–180.

42 Cao, Y., Fatemi, V., Fang, S. et al. (2018). Unconventional superconductivity in magic-angle graphene superlattices. *Nature* 556: 43–50.

43 Biscoe, J. and Warren, B.E. (1942). An X-ray study of carbon black. *J. Appl. Phys.* 13: 364–371.

44 Takaba, H., Omachi, H., Yamamoto, Y. et al. (2009). Selective synthesis of 12 cycloparaphenylene. *Angew. Chem.-Int. Ed.* 48: 6112–6116.

45 Yamago, S., Watanabe, Y., and Iwamoto, T. (2010). Synthesis of 8 cycloparaphenylene from a square-shaped tetranuclear platinum complex. *Angew. Chem.-Int. Ed.* 49: 757–759.

46 Kawasumi, K., Zhang, Q.Y., Segawa, Y. et al. (2013). A grossly warped nanographene and the consequences of multiple odd-membered-ring defects. *Nat. Chem.* 5: 739–744.

47 Mackay, A.L. and Terrones, H. (1991). Diamond from graphite. *Nature* 352: 762.

48 Lenosky, T., Gonze, X., Teter, M., and Elser, V. (1992). Energetics of negatively curved graphitic carbon. *Nature* 355: 333–335.

49 Nishihara, H., Simura, T., Kobayashi, S. et al. (2016). Oxidation-resistant and elastic mesoporous carbon with single-layer graphene walls. *Adv. Funct. Mater.* 26: 6418–6427.

50 Kudryavtsev, Y.P., Evsyukov, S.E., Guseva, M.B. et al. (1993). Carbyne – the third allotropic form of carbon. *Russ. Chem. Bull.* 42: 399–413.

51 Shi, L., Rohringer, P., Suenaga, K. et al. (2016). Confined linear carbon chains as a route to bulk carbyne. *Nat. Mater.* 15: 634–639.

52 Robertson, J. (1992). Properties of diamond-like carbon. *Surf. Coat. Technol.* 50: 185–203.

53 Vasudev, M.C., Anderson, K.D., Bunning, T.J. et al. (2013). Exploration of plasma-enhanced chemical vapor deposition as a method for thin-film fabrication with biological applications. *ACS Appl. Mater. Interfaces* 5: 3983–3994.

54 Tan, X., Li, J., Meng, K., and Zhai, H. (2023). Microstructures and visible-infrared optical properties of diamond-like carbon films deposited by magnetron sputtering. *Diam. Relat. Mater.* 133: 109724.

55 Li, Y., Xu, L., Liu, H., and Li, Y. (2014). Graphdiyne and graphyne: from theoretical predictions to practical construction. *Chem. Soc. Rev.* 43: 2572–2586.

56 Yue, Q., Chang, S., Kang, J. et al. (2013). Mechanical and electronic properties of graphyne and its family under elastic strain: theoretical predictions. *J. Phys. Chem. C* 117: 14804–14811.

57 Ohtani, S. (1997). *Tanso Jimon Jitou [in Japanese]*. Shoukabou.

58 LeGe, N., He, X.-X., Wang, Y.-X. et al. (2023). Reappraisal of hard carbon anodes for practical lithium/sodium-ion batteries from the perspective of full-cell matters. *Energy Environ. Sci.* 16: 5688–5720.

59 Orikasa, H., Akahane, T., Okada, M. et al. (2009). Electrochemical behavior of carbon nanorod arrays having different graphene orientations and crystallinity. *J. Mater. Chem.* 19: 4615–4621.

60 Nishihara, H. and Kyotani, T. (2012). Templated nanocarbons for energy storage. *Adv. Mater.* 24: 4473–4498.